

# AN ANTISYMMETRIC SOLUTION OF THE 3D INCOMPRESSIBLE NAVIER-STOKES EQUATIONS

C. Boldrighini \*

S. Frigio †

P. Maponi ‡

A. Pellegrinotti §

Ya. G. Sinai ¶

November 7, 2019

## Abstract

We report results on the behavior of a particular incompressible Navier-Stokes (NS) flow in the whole space  $\mathbb{R}^3$ , related to the complex singular solutions introduced by Li and Sinai in [13] that blow up at a finite time. The flow exhibits for some time a tornado-like behavior: a sharp increase of vorticity and of the maximal velocity, with concentration in an annular region around an axis. There is however no rotation around the axis and the approximate axial symmetry with no swirl excludes a real blow-up. We conclude with a discussion on the possible candidates for a real blow-up.

Keywords: Incompressible Navier-Stokes, Singular solutions, Blow-up, Tornadoes

## 1 Introduction

We report results, obtained by computer simulations, guided by a theoretical analysis, on a new solution of the incompressible Navier-Stokes equations (NS) in  $\mathbb{R}^3$ , with no boundary conditions, which arises in connection with the contribution of Li and Sinai [13] to the “global regularity problem”, i.e., the problem whether smooth solutions in absence of forcing can become singular at a finite time. The problem is open since the pioneering work of J. Leray [11] in 1937, and, in spite of many brilliant contributions, it is still open and in the list of the Clay millennium prize. Mathematically speaking the most notable difficulties of NS equations in 3D are its non-locality, due to incompressibility, and super-criticality. The system is super-critical with respect to the basic energy conservation law.

Leray, who first proved a global weak existence theorem and a uniqueness and regularity theorem only for finite times, believed that there is loss of regularity and it is related to turbulence. The modern view of turbulence involves transitions to chaotic flows rather than singularities. However, if singularities exist, they could describe sudden concentrations of energy in a finite region, as it happens in tornadoes or hurricanes, for which no effective model is now available. In fact, the main features of the possible finite-time singularities (“blow-up”), are the divergence of the total enstrophy [19], and the divergence at some point of the absolute value of the velocity [17].

In recent times, results of discrete models of the NS equations which preserve the energy conservation [6, 9] seem to indicate that blow-up’s are real. A blow-up was also proved by T. Tao [18] for a continuous

---

\*Istituto Nazionale di Alta Matematica, Università di Roma Tre, Largo S. Leonardo Murialdo 1, 00146 Rome, Italy.

†Scuola di Scienze e Tecnologie, Università di Camerino, 62932 Camerino, Italy.

‡Scuola di Scienze e Tecnologie, Università di Camerino, 62932 Camerino, Italy.

§Dipartimento di Matematica e Fisica, Università di Roma Tre, Largo S. Leonardo Murialdo 1, 00146 Rome, Italy. Partially supported by research funds of INdAM (G.N.F.M.), M.U.R.S.T. and Università Roma Tre.

¶Dept. of Mathematics, Princeton University and Russian Academy of Sciences

model obtained by modifying the bilinear term of the NS equations. (The introduction is a good review of the state of the global regularity problem.) As for the evidence from computer simulations, the NS equations are in general difficult to follow on the computer, especially for high values of the velocity and the vorticity, and in absence of reliable theoretical guide-lines on the structure of the blow-up the computer simulation are inconclusive (see, e.g., [8])

In 2008 a paper of Li and Sinai [13] introduced a new approach. It is based on dynamical system techniques, which allow to control, for some classes of flows, the transfer of energy to the fine scales. The approach can also be applied to other models [15]. We give here a brief description.

Consider the NSS in the whole space  $\mathbb{R}^3$  with no forcing

$$\frac{\partial \mathbf{u}}{\partial t}(\mathbf{x}, t) + \sum_{j=1}^3 u_j(\mathbf{x}, t) \frac{\partial \mathbf{u}}{\partial x_j}(\mathbf{x}, t) = \nu \Delta \mathbf{u}(\mathbf{x}, t) - \nabla p(\mathbf{x}, t), \quad \mathbf{x} = (x_1, x_2, x_3) \in \mathbb{R}^3. \quad (1)$$

$$\nabla \cdot \mathbf{u}(\mathbf{x}, t) = \sum_j \frac{\partial u_j}{\partial x_j}(\mathbf{x}, t) = 0, \quad \mathbf{u}(\mathbf{x}, 0) = \mathbf{u}_0(\mathbf{x}), \quad (2)$$

where  $\nu$  is the kinematic viscosity and  $p$  is the pressure, which can, by incompressibility, be recovered in terms of the velocity field by a Biot-Savart law. Assuming  $\nu = 1$  (which can always be obtained by a suitable scaling), and introducing the modified Fourier transform

$$\mathbf{v}(\mathbf{k}, t) = \frac{i}{(2\pi)^3} \int_{\mathbb{R}^3} \mathbf{u}(\mathbf{x}, t) e^{-i(\mathbf{k}, \mathbf{x})} d\mathbf{x}, \quad \mathbf{k} = (k_1, k_2, k_3) \in \mathbb{R}^3, \quad (3)$$

where  $\langle \cdot, \cdot \rangle$  denotes the scalar product in  $\mathbb{R}^3$ , the equation (1) can be written, by a Duhamel formula, as a single integral equation:

$$\mathbf{v}(\mathbf{k}, t) = e^{-t\mathbf{k}^2} \mathbf{v}_0(\mathbf{k}) + \int_0^t e^{-(t-s)|\mathbf{k}|^2} \int_{\mathbb{R}^3} \langle \mathbf{v}(\mathbf{k} - \mathbf{k}', s), \mathbf{k} \rangle P_{\mathbf{k}} \mathbf{v}(\mathbf{k}', s) d\mathbf{k}' ds, \quad (4)$$

where  $P_{\mathbf{k}} \mathbf{v} = \mathbf{v} - \frac{\langle \mathbf{v}, \mathbf{k} \rangle}{|\mathbf{k}|^2} \mathbf{k}$  denotes the solenoidal projector and  $\mathbf{v}_0$  is the transform of  $\mathbf{u}_0$ . In general  $\mathbf{v}(\mathbf{k}, t)$  is a complex function. Li and Sinai consider only real solutions of (4), which in general correspond to complex solutions of (1). However if  $\mathbf{v}_0(\mathbf{k})$  (and hence  $\mathbf{v}(\mathbf{k}, t)$  for  $t > 0$ ) is antisymmetric, the solution  $\mathbf{u}(\mathbf{x}, t)$  is also real and antisymmetric in  $\mathbf{x}$ .

Multiplying the initial data by a real parameter  $A$ , which controls the initial energy, and iterating the Duhamel formula, the solution of (4) is written as a power series:

$$\mathbf{v}_A(\mathbf{k}, t) = A \mathbf{g}^{(1)}(\mathbf{k}, t) + \int_0^t e^{-\mathbf{k}^2(t-s)} \sum_{p=2}^{\infty} A^p \mathbf{g}^{(p)}(\mathbf{k}, s) ds, \quad (5)$$

where  $\mathbf{g}^{(1)}(\mathbf{k}, s) = e^{-s\mathbf{k}^2} \mathbf{v}_0(\mathbf{k})$ ,  $\mathbf{g}^{(2)}(\mathbf{k}, s) = \int_{\mathbb{R}^3} \langle \mathbf{g}^{(1)}(\mathbf{k} - \mathbf{k}', s), \mathbf{k} \rangle P_{\mathbf{k}} \mathbf{g}^{(1)}(\mathbf{k}', s) d\mathbf{k}'$  and for  $p > 2$

$$\begin{aligned} \mathbf{g}^{(p)}(\mathbf{k}, s) = & \sum_{\substack{p_1+p_2=p \\ p_1, p_2 > 1}} \int_0^s ds_1 \int_0^s ds_2 \int_{\mathbb{R}^3} \langle \mathbf{g}^{(p_1)}(\mathbf{k} - \mathbf{k}', s_1), \mathbf{k} \rangle \\ & \cdot P_{\mathbf{k}} \mathbf{g}^{(p_2)}(\mathbf{k}', s_2) e^{-(s-s_1)(\mathbf{k}-\mathbf{k}')^2 - (s-s_2)(\mathbf{k}')^2} d\mathbf{k}' + \text{boundary terms}. \end{aligned} \quad (6)$$

The boundary terms involve  $\mathbf{g}^{(1)}$  and have a slightly different form (see, e.g., [4], where it is also shown, under some general conditions on  $\mathbf{v}_0$ , that the series converges if  $|A|t$  is small).

Li and Sinai [13] consider real initial data  $\mathbf{v}_0$  such that the support is mainly concentrated inside a sphere  $K_R$  of radius  $R$  centered around the point  $\mathbf{k}^{(0)}$  with  $|\mathbf{k}^{(0)}| \gg R$ . Then the function  $\mathbf{g}^{(p)}$ , which is essentially a convolution, has a support centered around  $p\mathbf{k}^{(0)}$  and (by analogy with probability theory) an effective diameter of the order  $\mathcal{O}(\sqrt{p})$ .

Li and Sinai argue that the behavior of  $\mathbf{g}^{(p)}$  for large  $p$  is determined by the fixed points of the map  $\tilde{\mathbf{g}}^{(p)} \rightarrow \tilde{\mathbf{g}}^{(p+1)}$ , where  $\tilde{\mathbf{g}}^{(p)}(\mathbf{Y}, s) = \mathbf{g}^{(p)}(p\mathbf{k}^{(0)} + \sqrt{p}\mathbf{Y}, s)$  are the functions in the rescaled variables

(rescaled as for the Central Limit Theorem). Hence, if we know the fixed point corresponding to the initial data we can control the excitation of the high  $\mathbf{k}$ -modes, i.e., of the fine structure components of  $\mathbf{u}(\mathbf{x}, t)$ .

More precisely, in [13] the following *Ansatz* is formulated: for a class of gaussian dominated initial data with support as described above, as  $p \rightarrow \infty$  the following asymptotics holds

$$\tilde{\mathbf{g}}^{(p)}(\mathbf{Y}, s) \sim p(\Lambda(s))^p \prod_{i=1}^3 g(Y_i)(\mathbf{H}(\mathbf{Y}) + \delta^{(p)}(\mathbf{Y}, s)), \quad \mathbf{Y} = (Y_1, Y_2, Y_3) \quad (7)$$

where  $\mathbf{H}$  is the fixed point,  $g(x) = \frac{e^{-\frac{x^2}{2}}}{\sqrt{2\pi}}$  is the standard Gaussian density,  $\Lambda$  is a strictly increasing smooth positive function and  $\delta^{(p)}(\mathbf{Y}, s) \rightarrow 0$  as  $s \rightarrow \infty$ . (Assuming the standard gaussian is not restrictive, as it can always be obtained by rescaling.) The fixed point equation for  $\mathbf{H}$  [13, 5, 3] has infinitely many solutions that can be explicitly written down [13]. ( $\mathbf{H}$  is in fact a plane vector, as its component along  $\mathbf{k}^{(0)}$  vanishes by incompressibility.)

Assuming  $\mathbf{k}^{(0)} = (0, 0, a)$ , with  $a > 0$ , the *Ansatz* (7) is proved in [13] for the fixed point  $\mathbf{H}^{(0)}(\mathbf{Y}) = c(Y_1, Y_2, 0)$ , where  $c$  is a real constant. It turns out that the linearized map at the fixed point has a 6-dimensional unstable subspace and a 4-dimensional neutral subspace, in addition to an infinite-dimensional stable one. The main result of [13] can be formulated as follows. Let  $a > b \gg 1$ , and consider initial data of the form

$$\mathbf{v}_0(\mathbf{k}) = \bar{\mathbf{v}}(\mathbf{k}) = A \left[ \left( k_1, k_2, -\frac{k_1^2 + k_2^2}{k_3} \right) + \Phi(k_1, k_2, k_3) \right] \prod_{i=1}^2 g(k_i) g(k_3 - a) \chi_b(k_3 - a), \quad (8)$$

where  $\chi_b(k_3)$  is smooth and such that  $\chi_b(k_3) = 0$  if  $|k_3| \geq b$ ,  $\chi_b(\mathbf{k}) = 1$  if  $|\mathbf{k}| \leq b - \epsilon$ , with  $\epsilon$  small enough,  $\Phi = \Phi^{(1)} + \Phi^{(2)}$ ,  $\Phi^{(1)}$  is a linear combination of the unstable and neutral eigenfunctions of the linearized map near  $\mathbf{H}^{(0)}$ , and  $\Phi^{(2)}$  is a vector in the stable subspace. Then if  $\Phi^{(2)}$  is small enough, there are a time interval ( $S_- \leq s \leq S_+$ ) and an open set of the parameters defining  $\Phi^{(1)}$  for which the *Ansatz* (7) holds.

The blow-up is an easy consequence: if  $A = \pm \frac{1}{\Lambda(\tau)}$ ,  $\tau \in (S_-, S_+)$ , the series (5) diverges as  $s \uparrow \tau$ . Observe that both the total enstrophy and the total energy diverge as  $t \uparrow \tau$  (for complex function the energy equality holds but it is not coercive).

Coming back to real flows, it is natural to consider initial data obtained by antisymmetrizing the data (8) associated to solutions that blow-up. Their support is now concentrated in two finite regions around  $\pm \mathbf{k}^{(0)}$ , and the convolution  $\mathbf{g}^{(p)}$  is a sum of terms centered around the points  $(0, 0, \ell a)$  with  $\ell = -p, \dots, p$ , with the main contribution coming for  $|\ell| = \mathcal{O}(\sqrt{p})$ . We have again a simple mechanism which, as the components  $\mathbf{g}^{(p)}$  are excited, moves the support of the solution to the high  $\mathbf{k}$  region. It is weaker than for the complex case, but it is rather efficient, especially if  $a$  is large.

The present paper is a brief report on the behavior of one such solution, which exhibits some features of a ‘‘tornado’’, such as a sharp increase of the absolute values of velocity and vorticity in a confined region, but does not seem to blow up. As we argue below, this is possibly due to the axial symmetry of the fixed point  $\mathbf{H}^{(0)}$ . We expect however that the results of [13] on the blow-up hold also for other fixed points  $\mathbf{H} \neq \mathbf{H}^{(0)}$ , which are in general not axial symmetric, and we are sure that. In absence of theoretical results, important information can be obtained on the complex flows and their related real flows by computer simulations, which can also reveal physically relevant details.

From the mathematical point of view one should extend the fixed point analysis to the real antisymmetric solutions, and also extend the whole theory to other fixed points  $\mathbf{H} \neq \mathbf{H}^{(0)}$ .

The plan of our paper is as follows. In §2 we give some results of computer simulations, and §3 is devoted to concluding remarks.

## 2 Results of computer simulations

The initial data of the real flow are obtained by antisymmetrizing the function (8) with  $\Phi \equiv 0$  and  $A > 0$  (the simulations show that  $\Phi$  does not have much influence on the behavior of the solution):

$$\mathbf{v}^{(0)}(\mathbf{k}) = A \left( k_1, k_2, -\frac{k_1^2 + k_2^2}{k_3} \right) g(k_1)g(k_2) [g(k_3 - a)\chi_b(k_3 - a) + g(k_3 + a)\chi_b(k_3 + a)]. \quad (9)$$

We used a special program for solutions of the integral equation (4), created for the purpose of following the blow-up of the complex solutions, as described in the paper [3], where solutions of (4) with initial data of the type (8) could be followed up to times close to the critical blow-up time.

Our mesh in  $\mathbf{k}$ -space is a regular lattice centered at the origin with step  $\delta = 1$ , with maximal configuration  $[-254, 254] \times [-254, 254] \times [-3000, 3000]$ . We deal with about  $5 \cdot 10^9$  real numbers, close to the maximal capacity of modern supercomputers.

As in the previous work [3], our aim was to follow the behavior of the total enstrophy and of its marginal distributions in  $\mathbf{k}$ -space, which describes the flow of energy to the microscale in physical space. The mesh step  $\delta = 1$  allows to follow the solution for values of  $|\mathbf{k}|$  of a few thousand. The behavior of the total enstrophy and its marginals in  $\mathbf{k}$ -space is stable with respect to refinements of the mesh, as it is mainly due to the extension of the support along the  $k_3$ -axis (the transversal diameter of the support grows more slowly). On the other hand the mesh step is rough for the initial values (9), which have a diameter of the essential support of the order of a few units, so that the large scale behavior of the solution  $\mathbf{u}(\mathbf{x}, t)$  is poorly reproduced, as it happens with the axial symmetry (as it happens for the axial symmetry in some figures below). An analysis comparing the accuracy of our program with respect to that of finite-difference methods is under way.

We report results obtained by simulating a particular solution with initial data (9):  $a = 30$  and  $A$  is such that the initial energy  $E_0 = \frac{1}{2} \int_{\mathbb{R}^3} |\mathbf{u}(\mathbf{x}, t)|^2 d\mathbf{x} = 2.5 \times 10^5$ . The study of the behavior of the solutions as the parameters  $a$  and  $A$  vary is under way. Recall however that the NS scaling holds: If  $\mathbf{v}(\mathbf{k}, t)$  is a solution of (4) with initial data  $\mathbf{v}_0(\mathbf{k})$ , and  $\lambda > 0$  then the function  $\mathbf{v}^{(\lambda)}(\mathbf{k}, t) = \lambda^2 \mathbf{v}(\lambda \mathbf{k}, \lambda^{-2} t)$  is also a solution with initial data  $\lambda^2 \mathbf{v}_0(\lambda \mathbf{k})$ .

In what follows time is measured in units of  $\tau = 1.5625 \times 10^{-8}$ . As for the complex case [3] the large initial data ensure a short running time, which makes simulations possible.

The first remarkable feature of the flow is that the total enstrophy  $S(t) = \int_{\mathbb{R}^3} |\omega(\mathbf{x}, t)|^2 d\mathbf{x}$ , where  $\omega(\mathbf{x}, t)$  is the vorticity field, increases sharply up to a critical time  $T_E \approx 711\tau$  and then decays. The same pattern is followed by the maximal value of the speed  $|\mathbf{u}(\mathbf{x}, t)|$ , except that the critical value is  $T_V \approx 400\tau$ .

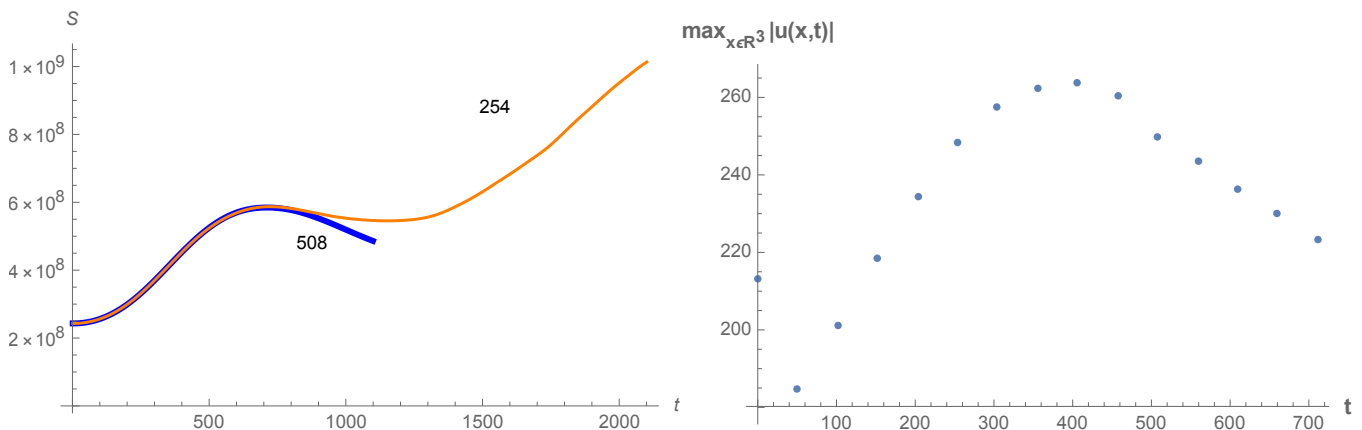


Figure 1: *Left side: Plot of the total enstrophy  $S(t)$  with mesh  $[-147, 147]^2 \times [-3000, 3000]$  (orange) and mesh  $[-254, 254]^2 \times [-3000, 3000]$  (blue). Right side: Plot of the maximal velocity as a function of time.*

In Fig. 1 (left) the blue line is a more precise description of the behavior of the total enstrophy. The orange line describes a “false blow-up” due to a spurious production of enstrophy at the boundary corresponding to the extremal values  $k_1, k_2 = \pm 147$  of the narrow mesh.

Fig. 2 below describes the evolution in time of the marginal densities of the enstrophy along the third axis: in  $\mathbf{k}$ -space (left)  $S_3(k_3, t) = \int_{\mathbb{R}^2} |\mathbf{k}|^2 |\mathbf{v}(\mathbf{k}, t)|^2 dk_1 dk_2$  (left), and in  $\mathbf{x}$ -space  $\tilde{S}_3(x_3, t) = \int_{\mathbb{R}^2} |\omega(\mathbf{x}, t)(\mathbf{x}, t)|^2 dx_1 dx_2$ .

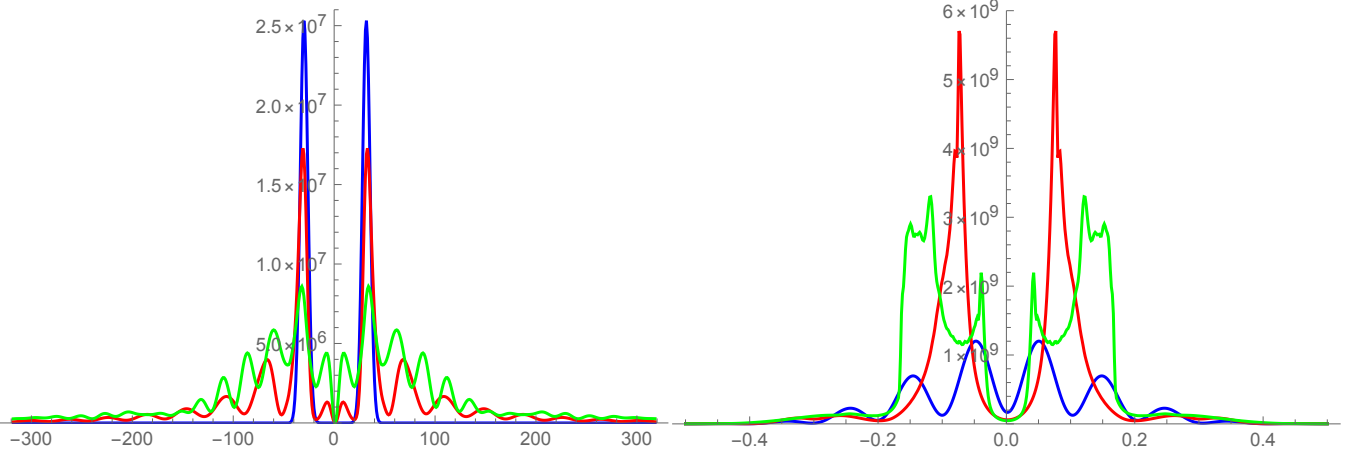


Figure 2: Plots of the marginal distributions  $S_3(k_3, t)$  (left) and  $\tilde{S}_3(x_3, t)$  (right) at the times  $t = 0$  (blue),  $t = 400\tau \approx T_V$  (red), and  $t = 711\tau \approx T_M$  (green).

On the left side of Fig.2 one can see how the support of the solution moves into the high  $|\mathbf{k}|$ -region. As predicted by the theory, as time grows the peaks of the figure on the left tend to be close to the values  $k_3 \approx ja$ , with  $j = \pm 1, \pm 2, \dots$  (green line), a modulated periodicity corresponding in the figure on the right to the peaks of the green line at  $x_3 = \pm \bar{x}_3$  with  $\bar{x}_3 \approx \frac{\pi}{a}$ .

The evolution of  $\tilde{S}_3(x_3, t)$  as illustrated by Fig. 2 also shows that the vorticity is concentrated in the neighborhood of symmetric pairs of planes orthogonal to the  $x_3$ -axis. This is also true for the large values of the velocity field  $\mathbf{u}(\mathbf{x}, t)$ , as shown by the following Fig. 3, where we report the absolute value of the velocity field on the plane  $x_3 = 0.08$ , corresponding to the right red peak on  $\tilde{S}_3(x_3, 400)$  of Fig. 2.

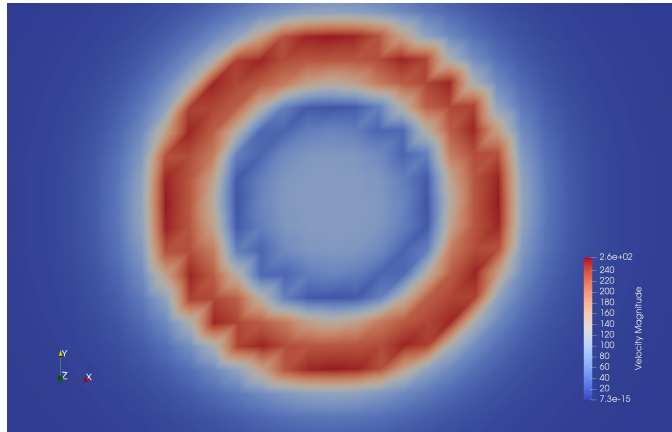


Figure 3: The absolute value velocity field  $|\mathbf{u}(\mathbf{x}, t)|$  on the plane  $x_3 = 0.03$  at the time  $t = 400\tau$ . The red color indicates the highest values.

Much interest has been devoted in recent times to the behavior of the angle between the velocity  $\mathbf{u}(\mathbf{x}, t)$  and the vorticity  $\omega(\mathbf{x}, t) = \nabla \times \mathbf{u}(\mathbf{x}, t)$  [1, 7]. In our case the average cosine of the angle, weighted

with the local energy  $\frac{|\mathbf{u}(\mathbf{x},t)|^2}{2}$ , is zero at the initial time (orthogonality) and increases up to the time  $T_E$ , when it reaches a value close to 0.45. The solution could not be followed after time  $T_E$  with enough accuracy (as it appears, it begins to decrease), so that we have no hint on whether “beltramization” [7] is taking place.

### 3 Concluding remarks

As shown by Figg. 1, 2, 3, up to the critical time  $T_V \approx 400\tau$  the maximal velocity has a significant increase, and the vorticity also grows and undergoes a sharp concentration in two “doughnuts” around the  $x_3$ -axis, bisected by the planes  $x_3 \approx \pm 0.8$ . The velocities are also maximal in the “doughnuts”, while elsewhere the fluid stays quiet. The total enstrophy increases up to the critical time  $T_M \approx 711\tau$ , while the maximal velocity decreases, and the sharp concentration persists, although the “doughnuts” undergo some deformation.

The description is strongly remindful of tornadoes and hurricanes, except perhaps that in our case there is no rotation around the  $x_3$ -axis. In fact the solution with initial data (9) is axial-symmetric with no swirl, although the axial symmetry is partially lost in Fig. 3 due to computation errors, as we explained above.

Concerning the global regularity problem, it is well-known that regularity for all times holds for axial symmetric solutions with no swirl and for solutions close to them [10]. As the fixed point  $\mathbf{H}^{(0)}$  is axial symmetric, the possible violations of symmetry and/or the initial swirl which can be introduced by inserting in the initial data (9) the function  $\Phi$  in (8) would not produce a singularity. As we said above, it is more promising to look at the real flows associated, again by antisymmetrization, to initial data related to fixed points  $\mathbf{H} \neq \mathbf{H}^{(0)}$  which are not axial symmetric. This will be the object of further work.

**Acknowledgements.** The computer simulations were performed at the Marconi Supercomputer of CINECA (Bologna, Italy), within the framework of a European PRACE Project n. 2015133169, and also of CINECA IS CRA Projects of type B and C.

### References

- [1] BEIRAO DA VEIGA (2012). Viscous incompressible flows under stress-free boundary conditions. The smoothness effect of near orthogonality and near parallelism between velocity and vorticity. *Bollettino B.U.M.I.* **V**, 225-232.
- [2] BOLDRIGHINI, C., FRIGIO, S. & MAPONI, P. (2012). Exploding solutions of the two-dimensional Burgers equations: Computer simulations. *J. Math. Phys.*, **53**, 083101.
- [3] BOLDRIGHINI, C., FRIGIO, S. & MAPONI, P. (2017): “On the blow-up of some complex solutions of the 3D Navier-Stokes Equations: theoretical predictions and computer simulation.” *IMA Journal of Mathematical Physics* vol. 83 pag 697-714; doi: 10.1063/1.4746814
- [4] BOLDRIGHINI, C., FRIGIO, S., MAPONI, P., PELLEGRINOTTI, A., SINAI, Ya.G.: “ Incompressible Navier-Stokes flows IN  $\mathbb{R}^3$  with tornado-like behavior”. Preprint (2019)
- [5] BOLDRIGHINI, C., LI, D. & SINAI, Ya., G. Ya. G. (2017): “Complex singular solutions of the 3-d Navier-Stokes equations and related real solutions”. *Journal of Statistical Physics*, vol. 167, n. 1, pagg. 1-13, DOI 10.1007/s10955-017-1730-1 (2017)
- [6] CHESKIDOV, A. (2008) Blow-up in finite time for the dyadic model of the Navier-Stokes equations. *Trans. Am. Math. Soc.*, **10**, 5101-5120.
- [7] FARHAT, A., GRUJIC, Z. (2019): Local Near-Beltrami Structure and Depletion of the Nonlinearity in the 3D Navier-Stokes Flows”. *Journal of Nonlinear Science* 29(2). DOI: 10.1007/s00332-018-9504-8

- [8] HOU, Th. Y. (2008) Blow-up or no blow-up? A unified computational and analytic approach to three-dimensional incompressible Euler and Navier-Stokes equations. *Acta Numerica*, **18**, 277-346.
- [9] KATZ, N. & PAVLOVIC, N. (2002) A cheap Caffarelli-Kohn-Nirenberg inequality for the Navier-Stokes equation with hyper-dissipation. *Geom. Funct. Anal.*, **12**, No. 2, 355-379.
- [10] LEI, Z. & ZANG, Q. (2017) “Criticality of the axially symmetric Navier-Stokes equations”. *Pacific Journal of Mathematics*, **289**, 169-187
- [11] LERAY, J. (1934) Sur le mouvement d’un liquide visqueux emplissant l’espace. *Acta Math* , **63**, 193-248.
- [12] TEMAM, R. (1979) *Navier-Stokes Equations*. North Holland.
- [13] LI, D. & SINAI, YA. G. (2008) Blowups of complex solutions of the 3D Navier-Stokes system and renormalization group method. *J. Eur. Math. Soc.*, **10**, 267-313.
- [14] LI, D, & SINAI, YA.G. (2010) Singularities of complex-valued solutions of the two-dimensional Burgers system. *J. Math. Phys.*, **51**, 01525.
- [15] LI, D, & SINAI, YA.G. (2010) Blowups of Complex-valued Solutions for Some Hydrodynamic models’. *Regular and Chaotic Dynamics*, **15**, Nos 4-5, 521-531.
- [16] RUZMAIKINA, A, & GRUJIC, Z. (2004) On Depletion of the Vortex-Stretching Term in the 3D Navier-Stokes Equations. *Comm. Math. Phys.*, **247** , 601-611.
- [17] SEREGIN, G. (2012) A Certain Necessary Condition of Potential Blow up for Navier-Stokes Equations. *Commun. Math. Phys.*, **312**, 833-845.
- [18] TAO, T. (2016) Finite time blowup for an averaged three-dimensional Navier-Stokes equation. *J. Amer. Math. Soc.* 29 (2016), no. 3, 601-674.
- [19] TEMAM, R. (1979) *Navier-Stokes Equations*. North Holland.